Li, Zhengmao; Kyyrä, Jorma; Xu, Yan; Zhao, Tianyang; Wang, Yunqi

Cooperative Operation of Renewable-Integrated Multi-Energy Microgrids Under Dynamic Rolling Horizon Strategy

Published in:
2023 25th European Conference on Power Electronics and Applications, EPE 2023 ECCE Europe

DOI:
10.23919/EPE23ECCEEurope58414.2023.10264441

Published: 01/01/2023

Document Version
Peer-reviewed accepted author manuscript, also known as Final accepted manuscript or Post-print

Please cite the original version:
Li, Z., Kyyrä, J., Xu, Y., Zhao, T., & Wang, Y. (2023). Cooperative Operation of Renewable-Integrated Multi-Energy Microgrids Under Dynamic Rolling Horizon Strategy. In *2023 25th European Conference on Power Electronics and Applications, EPE 2023 ECCE Europe* (2023 25th European Conference on Power Electronics and Applications, EPE 2023 ECCE Europe). IEEE.
https://doi.org/10.23919/EPE23ECCEEurope58414.2023.10264441

Cooperative Operation of Renewable-Integrated Multi-Energy Microgrids Under Dynamic Rolling Horizon Strategy

Li Zhengmao[a], Jorma Kyyrä[a], Xu Yan[b], Zhao Tianyang[c], Wang Yunqi[d]
a: Aalto University, School of Electrical Engineering, Espoo, Finland.
b: Nanyang Technological University, School of EEE, Singapore.
c: University of Bath, Department of Electronic & Electrical Engineering, Claverton, UK.
d: Monash University, Electrical, and Computer Systems Engineering, Melbourne, Australia.
Tel.: +358-504413955, +358-505639146, +65-6790 4508, +86-18611211209.
E-Mail : zhengmao.li@aalto.fi, jorma.kyyra@aalto.fi, xuyan@ntu.edu.sg, tz626@bath.ac.uk, yunqi.wang@monash.edu.

Keywords

«Energy management», «Energy storage», «Power-to-X», «Renewable energy systems», «Smart microgrids».

Abstract

In this paper, a cooperative operation method is proposed in a multi-energy microgrid with high penetration levels of renewable energy sources. To handle uncertainties rising from wind turbines and photovoltaic cells, the rolling optimization approach is thus applied to achieve online multi-energy management with the constantly updated information. Through the effective coordination of energy markets, multi-energy networks, energy storage systems, and generators, a reliable and economic operation scheme is fulfilled. At last, to show the effectiveness of our proposed method, a case study with two compassion cases for the operation of multi-energy microgrids is done. The simulation results indicate that our method is more cost-effective for the cooperative operation of renewable-integrated multi-energy microgrids under uncertainty sources.

1 Introduction

Currently, the increasing interaction of multiple energy carriers such as power, heat, gas, etc., facilitate the development of the multi-energy microgrid (MEMG), where various distributed generators, demand response schemes, as well as energy storage, are coordinated for effective multi-energy conversion [1]. In the meantime, for carbon-free generation, massive intermittent renewables are now gradually integrated into the MEMG which poses a significant threat to its operation reliability and economy. With this regard, tackling the negative effects of uncertain renewable generation and achieving effective multi-energy interactions become urgent tasks for optimal MEMG energy management [2].

In the literature, plenty of energy management research work has been conducted for MEMGs with high penetration levels of renewables. In [3], a coordinated supply method is presented for a MEMG to minimize its investment cost, energy consumption, CO2 emission, and energy supply risk at the same time. The study in [4] proposes a system-wide operation model for a MEMG to enhance its holistic energy utilization efficiency and operational flexibility via the integration of the heterogeneous energy storage system. Ref. [5] presents the techno-economic analysis model for a MEMG with a combined electric and thermal (heat and cooling) storage system to enhance operational flexibility as well as reduce the operation cost. In [6], an optimal cost minimization model is established for the MEMG with generators, energy storage, and demand response. All the units are coordinated for a more efficient and flexible operation. In [3]-[6], although effective energy management schemes are achieved, they assume that all the generators are located in the same place as the consumers. This is not practical as the real-world MEMG can be geographically large with coupled power and thermal networks for energy transmission [7].

To make the MEMG operation more practical, in [8], an optimal operation method for MEMGs is applied to reduce the operation cost. Coupling constraints of electrical and thermal networks and demand response are modeled. In [9], a dispatch strategy for the MEMG that utilizes the electricity and thermal network to realize multi-energy interactions is presented. The operation flexibility is greatly enhanced with lower cost. The research in [8]-[9] fully considers practical multi-energy network constraints, but the same as [3]-[6], they employ the forecast values of the renewable

generation as fixed inputs. However, renewable generation is highly intermittent and stochastic which will pose great adverse effects on the operation reliability and economy.

To address the uncertainties of renewables, the stochastic programming or robust optimization method is typically applied. In [10], an adaptive stochastic method is used to obtain operation decisions of MEMG with uncertain renewables. Via the coordination of multiple energy flows, the multi-energy supply cost is greatly reduced. Ref. [11] introduces a robust scheduling model for the MEMG with demand response and renewables to maximize the operating profit and reduce the customers' energy usage bills. The study in [12] uses the hybrid stochastic and robust optimization method to handle all system uncertainty sources for a both economic and reliable MEMG energy management scheme. Although uncertainties from renewables are handled in [10]-[12] via the day-ahead one-time forecast in their two-stage structures, the long lead-time forecast applied will not be accurate enough for real-time operation. In reality, the forecasting accuracy is much higher with the much shorter-term forecast [13]. In this way, it is meaningful and essential to make full use of updated forecasts for more optimal as well as practical operation solutions.

At last, all the MEMGs in [3]-[6] and [8]-[12] operate in the grid-tied mode to exchange power with the main grid as price takers. Nonetheless, with the deregulation of the electricity market [14], the MEMG, which owns an increasing market share now, can also impact power prices in the market via effective trading. As a result, the electricity market is no longer monopolized by the main grid and MEMGs can also be price makers. In addition, as there is no competition between a single MEMG and the main grid, the cooperative operation mode can be employed.

To fill in the above research gaps, in this paper, a rolling horizon-based operation approach is presented to achieve the cooperative operation of a MEMG with massive renewables as well as practical power and thermal networks, the main contributions are summarized below:

1) A practical MEMG operation model is built that considers the power and thermal networks, heterogeneous energy storage systems, power-to-thermal units, tri-generators, etc for effective multi-energy conversion. 2) To deal with the intermittency of renewable generation on a real-time (online) scale, the rolling horizon-based approach is applied to make full use of the constantly updated short lead-time forecast. 3) The cooperative trading mechanism is used for electricity transactions to facilitate the active MEMG participation in the power market and reduce energy supply costs.

2 Structure of Cooperative MEMG

2.1 Basic structure

The structure of a grid connected MEMG in the electricity market is shown in Fig. 1 [10]. The MEMG is built upon practical integrated power and thermal networks.

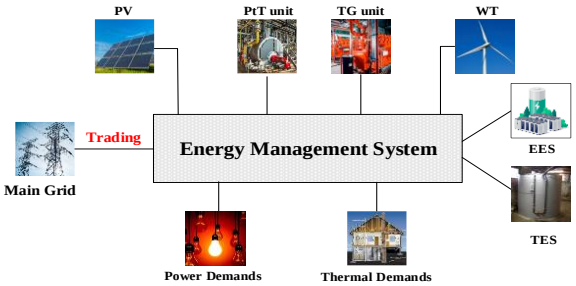

Fig. 1: Typical structure of the MEMG.

Various resources indicated below are deployed for the multi-energy supply in the MEMG:

1) Renewable generators: wind turbines (WTs) and photovoltaic cells (PVs) are used to produce electricity with high intermittency[11].

2) Tri-generators (TGs): they could produce power, heat, and cooling energy simultaneously for higher energy utilization efficiency [4].

3) Power-to-thermal (PtT) units: they are used to enhance multi-energy interaction [10].

4) Heterogeneous energy storage systems: they include electric energy storage (EES) and thermal energy storage (TES) for load leveling and energy shifting [8].

5) Energy trading with the main grid: all power surplus and deficiencies could be compensated via effective electricity trading [14]. Note that given the real market status, only the electricity market is considered and the thermal energy is generated and consumed locally [4].

2.2 Cooperative Trading Model

With the restructuring of electricity markets, the MEMG can also impact the final power prices, that is, rather than a sole price taker, it is now transformed into a price maker [15]. Given the relationship between the MEMG and the main grid, the cooperative pricing mechanism in (1) [14] could be used to indicate this cooperative trading relationship:

$$\delta_e^t = \delta_{\mathrm{bp,e}}^{\mathrm{t}} - \delta_{\mathrm{bp,e}}^{\mathrm{t}} \cdot P_{ts}^t / \mathrm{P}_{\mathrm{ts}}^{\mathrm{cap}} \qquad (1)$$

where δ_e^t is the final power price; $\delta_{\text{in,e}}^{\text{t}}$ is the base time-of-use prices set by the main grid. P_{ts}^t is the electricity trading quantity; $\text{P}_{\text{ts}}^{\text{cap}}$ is the market trading capacity.

The pricing mechanism in (1) shows that the final price can be related to the trading quantity of the MEMG. It constitutes an effective means to describe the cooperative game between the MEMG and the main grid. Besides, when P_{ts}^t is positive (sell), the final prices are lower than the bases and when P_{ts}^t is negative (buy), the final prices are higher. This is rational as it facilitates the MEMG to use local resources as its priority rather than external trading.

3 Problem Formulation for the Cooperative MEMG Operation

3.1 Objective

The goal of the MEMG cooperative operation is to minimize the total multi-energy supply cost under interactive energy trading [16] as below:

$$min\, C_{to} = \sum_{t\in \text{N}^{\text{T}}} [\underbrace{C_{gc}^t \Delta \text{t}}_{Generation\,Cost} - \underbrace{B_{tr}^t \Delta \text{t}}_{Trading\,Revenue}] \quad (2)$$

where C_{to} is the total multi-energy supply cost; t is the index for operation interval; N^{T} means the total number of operation intervals; Δt is the unit interval; C_{gc}^t is the energy generation cost; B_{tr}^t is the revenue from the energy trading.

From (2), it can be seen the net energy supply cost is denoted as the differences between the generation cost and trading revenue.

$$B_{tr}^t = \delta_e^t P_{ts}^t = \delta_{\text{bp,e}}^{\text{t}} P_{ts}^t - \delta_{\text{bp,e}}^{\text{t}} (P_{ts}^t)^2 / \text{P}_{\text{ts}}^{\text{cap}} \quad (3)$$

Eq.(3) denotes that the trading revenue can be formulated as the multiplication of final trading prices and quantities;

$$C_{gc}^t = \sum_{k\in \text{N}^{\text{K}}} F_{fc}^{t,k} + F_{mc}^{t,k} + F_{dc}^{t,k} \quad (4)$$

$$F_{fc}^{t,k} = \lambda_{\text{ng}} P_{tg}^{t,k} / \eta_{\text{tg}}^{\text{e}} \quad (5)$$

$$F_{mc}^{t,k} = \begin{bmatrix} \lambda_{\text{ees}} (P_{esc}^{t,k} + P_{esd}^{t,k}) + \lambda_{\text{tes}} (Q_{tsc}^{t,k} + Q_{tsd}^{t,k}) + \\ \lambda_{\text{wt}} P_{wt}^{t,k} + \lambda_{pv} P_{pv}^{t,k} + \lambda_{cg} P_{cg}^{t,k} + \lambda_{PtT} P_{PtT}^{t,k} \end{bmatrix} \quad (6)$$

$$F_{dc}^{t,k} = \lambda_{dc} (P_{esc}^{t,k} + P_{esd}^{t,k}) \quad (7)$$

where k means the index for buses in the power network; N^{K} is the total number of buses; $F_{fc}^{t,k}$ is the fuel cost; $F_{mc}^{t,k}$ is the maintenance cost; $F_{dc}^{t,k}$ is the degradation cost of the EES; λ_{ng} is the fuel price; $P_{tg}^{t,k}$ is the power output of the TG; $\eta_{\text{tg}}^{\text{e}}$ is the electrical efficiency of the TG; λ_{ees}, λ_{tes}, λ_{wt}, λ_{pv}, λ_{tg} and λ_{PtT} are the unit maintenance cost of EES, TES, PV, WT, TG, and PtT unit; $P_{esc}^{t,k}$ and $P_{esd}^{t,k}$ mean the ESS charging and discharging power; $Q_{tsc}^{t,k}$ and $Q_{tsd}^{t,k}$ are the TES absorbing and releasing power; $P_{wt}^{t,k}$ and $P_{pv}^{t,k}$ is the power generation of WTs and PVs; $P_{PtT}^{t,k}$ is the power consumption of the PtT unit; λ_{dc} is the unit ESS degradation cost.

Eq.(4) obtains the generation cost, including the fuel cost (5), maintenance cost (6) , and the EES degradation cost in (7). Note that as the TES is usually in the form of tanks with no chemical process, its degradation cost is ignored [10].

3.2 Constraints

The MEMG operation constraints include the power flow, thermal flow, and operation limits for all distributed resources as below [8]:

a) Power flow model

$$P_{ap}^{t,b+1} = \begin{bmatrix} P_{ap}^{t,b} - P_{ac}^{t,b_0} - \text{P}_{\text{el}}^{\text{t,k}} + P_{wt}^{t,k} + \\ P_{pv}^{t,k} + P_{esd}^{t,k} - P_{esc}^{t,k} + P_{tg}^{t,k} - P_{PtT}^{t,k} \end{bmatrix} \quad (8)$$

$$P_{ap,\text{min}}^b \le P_{ap}^{t,b} \le P_{ap,\text{max}}^b \quad (9)$$

$$Q_{rp}^{t,b+1} = Q_{rp}^{t,b} - Q_{rp}^{t,b_0} - \text{Q}_{\text{rl}}^{\text{t,k}} \quad (10)$$

$$Q_{rp,\text{min}}^b \le Q_{rp}^{t,b} \le Q_{rp,\text{max}}^b \quad (11)$$

$$V_{bs}^{t,k} = V_{bs}^{t,k-1} - (\text{r}^{\text{b}} P_{ap}^{t,b} + \text{x}^{\text{b}} Q_{rp}^{t,b}) / \text{V}_{\text{sub}} \quad (12)$$

$$\text{V}_{\text{bs}}^{\text{min}} \le V_{bs}^{t,k} \le \text{V}_{\text{bs}}^{\text{max}} \quad (13)$$

where b is the index for branches which denote the power flow from different buses; $P_{ap}^{t,b}$ is the active power flow; b_0 means the lateral buses; $\text{P}_{\text{el}}^{\text{t,k}}$ means the active power loads [10]; $P_{ap,\text{min}}^b$ and $P_{ap,\text{max}}^b$ are the minimal and maximal active power flow limits; $Q_{rp}^{t,b}$ is the reactive power flow; $\text{Q}_{\text{rl}}^{\text{t,k}}$ shows the reactive power loads; $Q_{rp,\text{min}}^b$ and $Q_{rp,\text{max}}^b$ denote the minimal and maximal reactive power limits; $V_{bs}^{t,k}$ means the bus voltage; r^{b} and x^{b} are the line resistance and reactance; V_{sub} is the substation voltage; $\text{V}_{\text{bs}}^{\text{min}}$ and $\text{V}_{\text{bs}}^{\text{max}}$ are the minimal and maximal bus voltage.

Eqs. (8)-(13) are the *Linear Dist-flow* model of the power system which is widely used in the

literature [16]. It calculates the power flow that includes the active and reactive power balance and limits in (8)-(11), the relationship between voltage and power in (12), and the voltage safe ranges in (13) [8].

b) Thermal flow model

$$T_{s/r}^{t,m} = T_{s/r,(+)}^{t,p} \quad (14)$$

$$\sum_{p\in \boldsymbol{P}_{s/r,(-)}^{m}} T_{s/r,(-)}^{t,p} m_{s/r}^{t,p} = T_{s/r}^{t,m}\left(\sum_{p\in \boldsymbol{P}_{s/r,(+)}^{m}} m_{s/r}^{t,p}\right) \quad (15)$$

$$H_{s/r,(-)/(+)}^{t,p} = C_W m_{s/r}^{t,p} T_{s/r,(-)/(+)}^{t,p} \quad (16)$$

$$T_{s/r,(-)/(+)}^{min} \le T_{s/r,(-)/(+)}^{t,p} \le T_{s/r,(-)/(+)}^{max} \quad (17)$$

$$H_{tl}^{t,p} = C_W\left[m_s^{t,p} T_{s/r,(+)}^{t,p} - m_r^{t,p} T_{s/r,(-)}^{t,p}\right] \quad (18)$$

$$H_{tl}^{t,p} = H_{tg}^{t,k} + H_{PtT}^{t,k} + P_{ted}^{t,k} - P_{tec}^{t,k} \quad (19)$$

where m is the index for nodes, p is the index for pipes; $T_{s/r}^{t,m}$ denotes the node temperature of supply/return pipes; $T_{s/r,(+)}^{t,p}$ is the temperature at the start of the pipe; $\boldsymbol{P}_{s/r,(-)}^{m}$ is the set of pipe ends whose water flows into node m; $T_{s/r,(-)}^{t,p}$ is the temperature at the pipe end; $m_{s/r}^{t,p}$ is the mass flow rate of the water flowing in the pipe; $\boldsymbol{P}_{s/r,(+)}^{m}$ means the set of pipe starts whose water flows out of node m; $H_{s/r,(-)/(+)}^{t,p}$ is the thermal energy at the start/end of supply/return pipes; C_W is the water thermal capacity; $T_{s/r,(-)/(+)}^{min}$ and $T_{s/r,(-)/(+)}^{max}$ denote the minimal and maximal temperature of supply/return pipes; $H_{tl}^{t,p}$ is the thermal load; $H_{tg}^{t,k}$ and $H_{PtT}^{t,k}$ are the thermal generation from the TG unit and PtT unit.

The thermal flow is shown in (14)-(19) [10], in which (14) indicates that the temperature at the pipe start is the same as its connected node; (15) formulates the nodal temperature mix according to the *First Law of Thermo-Dynamics*; (16) gets the thermal energy in each pipe; (17) gives the safe range of the water temperature in the pipe; (18) means that the total thermal loads are denoted by thermal energy differences between the supply pipe start and return pipe end; (19) shows that thermal loads should be satisfied by all distributed thermal resources.

Note that according to [8], on the one hand, the constant mass flow but the variable temperature strategy is applied in this study, in this way, the thermal flow model is linear. On the other hand, given the pipe length, it needs time for water to flow from sources to nodes. Under the constant mass flow but variable temperature strategy, the time delay makes some thermal energy in the pipe come from generations of former time slots rather than the current time.

c) Operation of distributed resources

$$[P_{PtT}^{min,k}, P_{tg}^{min,k}] \le [P_{PtT}^{t,k}, P_{tg}^{t,k}] \le [P_{PtT}^{max,k}, P_{tg}^{max,k}] \quad (20)$$

$$[H_{tg}^{t,k}, H_{PtT}^{t,k}] = [\eta_{tg}^{h}, \eta_{PtT}^{h}]\cdot[P_{tg}^{t,k}, P_{PtT}^{t,k}] \quad (21)$$

where $P_{PtT}^{min,k}$ and $P_{PtT}^{max,k}$ mean the minimal and maximal energy input for the PtT unit; $P_{tg}^{min,k}$ and $P_{tg}^{max,k}$ are the minimal and maximal power output of the TG unit; η_{tg}^{h} and η_{PtT}^{h} mean the power to the thermal conversion efficiency of the TG unit and PtT unit.

The power generation of the TG unit and power consumption of the PtT unit is constrained in (20) ; the multi-energy conversion of both units is denoted in (14) [12].

$$[0,0] \le [P_{esc}^{t,k}, P_{esd}^{t,k}] \le [P_{esc}^{max,k} U_{esc}^{t,k}, P_{esd}^{max,k} U_{esd}^{t,k}] \quad (22)$$

$$U_{esc}^{t,k} + U_{esd}^{t,k} \le 1 \quad (23)$$

$$E_{ees}^{t,k} = (1-\kappa_{ees}^{k}) E_{ees}^{t-1,k} + (P_{esc}^{t,k}\eta_{esc}^{k} - P_{esd}^{t,k}/\eta_{esd}^{k})\Delta t \quad (24)$$

$$E_{ees}^{min,k} \le E_{ees}^{t,k} \le E_{ees}^{max,k} \quad (25)$$

where $P_{esc}^{max,k}$ and $P_{esd}^{max,k}$ denote the maximal charging and discharging power of the EES; $U_{esc}^{t,k}$ and $U_{esd}^{t,k}$ are the binary statuses for the charging and discharging; $E_{ees}^{t,k}$ is the stored energy; κ_{ees}^{k} is the self-decay rate of the EES; η_{esc}^{k} and η_{esd}^{k} are the charging and discharging efficiency; $E_{ees}^{min,k}$ and $E_{ees}^{max,k}$ are the minimal and maximal stored energy.

Eqs. (22)-(25) denote operation limits of EESs, including the charging and discharging power limit in (22), the non-simultaneous charging and discharging in (23); the energy balance condition of the ESS in (24), and EES energy capacity limits in (25) [4], [12].

$$[0,0] \le [H_{tsc}^{t,k}, H_{tsd}^{t,k}] \le [H_{tsc}^{max,k} U_{tsc}^{t,k}, H_{tsd}^{max,k} U_{tsd}^{t,k}] \quad (26)$$

$$U_{tsc}^{t,k} + U_{tsd}^{t,k} \le 1 \quad (27)$$

$$E_{tes}^{t,k} = (1-\kappa_{tes}^{k}) E_{tes}^{t-1,k} + (H_{tsc}^{t,k}\eta_{tsc}^{k} - H_{tsd}^{t,m,k}/\eta_{tsd}^{k})\Delta t \quad (28)$$

$$E_{tes}^{min,k} \le E_{tes}^{t,k} \le E_{tes}^{max,k} \quad (29)$$

where $H_{tsc}^{max,k}$ and $H_{tsd}^{max,k}$ denote the maximal absorbing and releasing power of the TES; $U_{tsc}^{t,k}$ and $U_{tsd}^{t,k}$ are binary statuses for the absorbing and releasing; $E_{tes}^{t,k}$ is the stored energy; κ_{tes}^{k} is the

TES self-decay rate; η_{tsc}^{k} and η_{tsd}^{k} are the absorbing and releasing efficiency; $E_{tes}^{min,k}$ and $E_{tes}^{max,k}$ are the minimal and maximal stored energy.

Similar to the EES, the operation limits of TES are given in (26)-(29) [6].

$$-P_{ts}^{cap} \le P_{ts}^{t} \le P_{ts}^{cap} \quad (30)$$

Eq. (30) means that the power transactions of the MEMG should be within a certain range [9].

3.3 Compact form

For better discussions, the MEMG cooperative operation model (2)-(30) is represented in the compact form as (31)-(33).

$$\min_{\mathbf{x}\in\Re_X} C_{to} = \mathbf{c}^T\mathbf{x} - \mathbf{x}^T\mathbf{Q}\mathbf{x} \quad (31)$$

$$s.t., \mathbf{A}\mathbf{x} \le \mathbf{f} \quad (32)$$

$$\mathbf{E}\mathbf{x} = \mathbf{d} \quad (33)$$

In (31), $\mathbf{c}^T\mathbf{x}$ denotes the linear generation cost in (4)-(7); the quadratic function $\mathbf{x}^T\mathbf{Q}\mathbf{x}$ means the benefit in (3). Vector $\mathbf{x}$ means all variables; $\Re_X$ is the feasible region of $\mathbf{x}$ indicated by (8)-(30); $\mathbf{c}$ and $\mathbf{Q}$ are the cost or benefit coefficients; $\mathbf{A}$ and $\mathbf{E}$ represent all coefficients of constraints; Vectors $\boldsymbol{f}$ and $\mathbf{d}$ mean the parameters set for all the inequality and equality constraints.

Note that, here the time dimension of Vector $\mathbf{x}$ is N^T, i.e., the whole operation interval. Besides, it can be observed that the MEMG cooperative operation model (31)-(33) is a mixed quadratic programming (MIQP) problem.

4 Solution Methodology for the Real-Time MEMG Operation

4.1 Basic mechanism

To make full use of the near-future forecasting information which is constantly updated in real time on the renewable generation from WTs and PVs as well as mitigate the adverse effects of their uncertainties on the system operation, the dynamic rolling horizon approach is used [13].

The rolling horizon approach is an optimization method that transforms one unified long open-loop optimization problem into a series of short closed-loop optimization ones using receding horizons. It is an online optimization method for handling uncertainties of renewable generation on a real-time scale [17].

In this study, the rolling horizon method has the following two main units:

i) **Prediction Unit**: There are different methods for the prediction of renewable generation such as the Kalman filter method, the time series approach, the neural network approach, etc. All predictions are inputs for the operation model and all the forecasting methods demonstrate a pattern that the shorter the lead time, the higher the forecast accuracy [13].

ii) **Rolling Horizon Unit**: The specific rolling horizon approach is denoted in Fig.2.

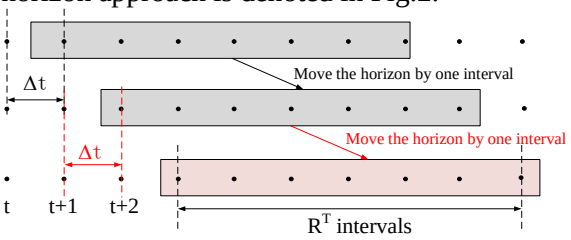

Fig. 2: Dynamic rolling horizon strategy

In every operation interval, the forecasts are conducted and utilized in the operation model to minimize the multi-energy supply cost over a certain horizon. Decisions for only the first next operation interval are finalized, and the horizon will move forward to the next interval [17].

4.2 Rolling horizon-based reformulation of the MEMG operation

Assume that the rolling horizon is R^T, then the MEMG cooperative operation problem in (31)-(33) can be reformulated as:

$$\min_{x^t\in\Re_X} C_{to}\big|_{t\in[t,t+R^T]} = \sum_{t}^{t+R^T} cx^t - q\cdot(x^t)^2 \quad (34)$$

$$s.t., ax^t \le f \quad (35)$$

$$ex^t = d \quad (36)$$

x^t indicates the decision at the interval t of the vector $\mathbf{x}$, c, q, a, f, e, and d mean the elements in the corresponding vectors.

In (34)-(36), the original large operation model in (31)-(33) is reformulated as a series of MIQP problems. Further, all MIQP problems can be efficiently solved by industry-proven efficient solvers like Cplex or Gurobi. Finally, it can be seen that the intermittency and stochasticity of renewable generation can be well handled via updated forecasts and optimization processes.

5 Case Study

5.1 Test system setup

In this study, the structure of the test MEMG is given in Fig.3. The studied MEMG is based on the IEEE 12-node distribution network and 11-node thermal network [18]. The MEMG is tied to

the main power grid, and trades with each other in the electricity market [4].

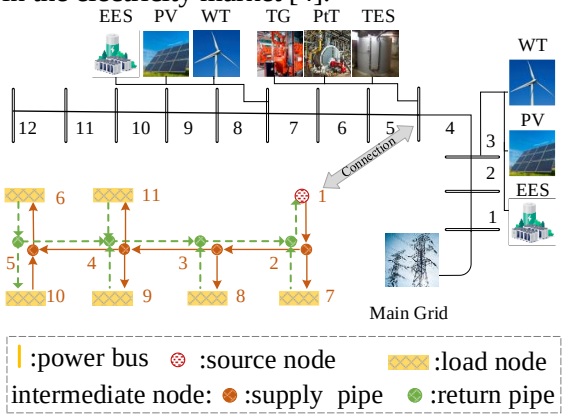

Fig. 3: The test MEMG with practical power and thermal networks

The MEMG configuration information in terms of the size and location of all internal units is given in Table I.

Table I: The MEMG configuration

Item/Bus(node)	3	4→1[a]	7
WT	100	-	200
PV	60	-	100
EES	50/200[b]	-	100/350[b]
TES	-	300\1000[b]	-
PtT unit	-	350	-
TG unit	-	600	-

[a]: The 1st number is the power bus index and the 2nd is the thermal node; [b]: The 1st number is the power capacity (kW) and the 2nd is the energy capacity (kWh) of energy storage; All numbers without superscripts mean the power capacity (kW)

The parameters for the MEMG operation in the cooperative mode are shown in Table II.

Table II: The MEMG operation parameters

η^{e}_{tg}	0.29	λ_{ng}	0.03578 $/kW
η^{h}_{tg}	1.26	κ^{k}_{ees}	0.0001
η^{h}_{PtT}	2.54	κ^{k}_{tes}	0.001
λ_{tg}	0.0032$/kW	λ_{PtT}	0.002 $/kW
λ_{tes}	0.0023$/kW	λ_{wt}	0.003$/kW
η^{k}_{esc} & η^{k}_{esd}	0.98	λ_{dc}	0.02 $/kW
η^{k}_{tsc} & η^{k}_{tsd}	0.95	λ_{ees}	0.001 $/kW

For the operation, the total horizon is set as one day (24 hours) with 1-hour granularity, and the rolling horizon is 12 hours with successively updated forecasts on the generation of WTs and PVs. For the MEMG, the substation voltage is set as 1.0 p.u., and the voltage limits of power buses are in the range of [0.95, 1.05] p.u [19]. More basic parameters regarding the power and thermal networks can be found in [16] and [19].

A winter case is studied here, where the power and heat demands need to be satisfied. The base power trading prices are shown in Fig. 4.

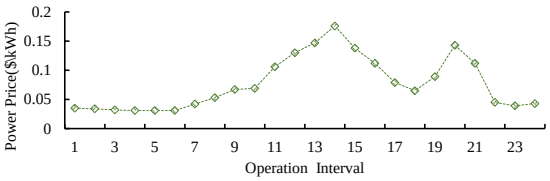

Fig. 4: The base electricity trading prices.

The power and heat loads are given in Fig.5.

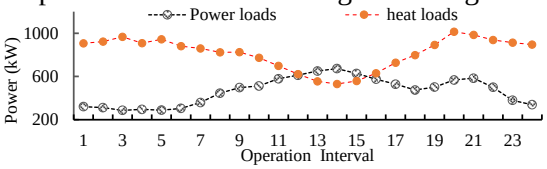

Fig. 5: The power and heat loads.

The base forecasts of renewable generation are given in Fig. 6-7 whose stochastic variations as 25% [10]. The temperature limits for supply and return pipes are [80,100] ℃ and [50, 70] ℃ [8].

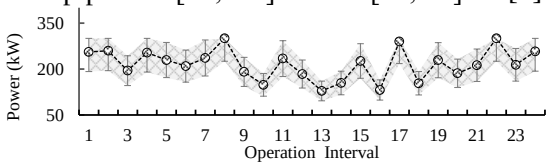

Fig. 6: The forecast of total WT generation with the stochastic variation range.

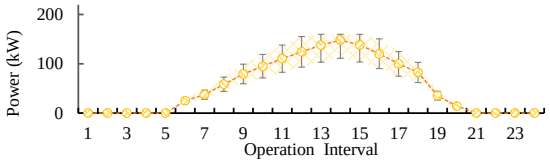

Fig. 7: The forecast of total PV generation with the stochastic variation range.

The case study is conducted on the General Algebraic Modelling System platform and then it is solved via the Cplex solver [14].

5.2 Simulation results

With 24 sets of 12-hour renewable forecasts, the rolling horizon strategy is employed. After the simulation, results for power and heat balance conditions are shown in Fig.8 and 9.

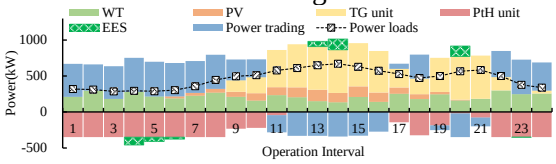

Fig. 8: The MEMG power balance condition.

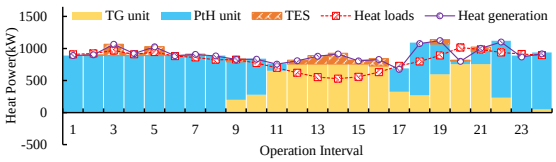

Fig. 9: The MEMG heat balance condition.

The power bidding prices after the cooperative MEMG operation are shown in Fig.10.

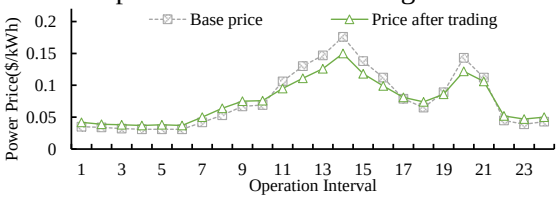

Fig. 10: The prices before and after trading.

From the energy balance conditions in Fig.8-9 and trading prices in Fig.10, the following can be observed:

i) All units i.e., the PtH unit, TG units, energy storage, and power transactions are coordinated for effective electricity and heat energy supply. Specifically, under low power trading prices (Fig.10 and 4, intervals 1-10 and 22-24), TG units are switched off, and most heat energy is produced via the PtH units (Fig.9, intervals 1-10 and 22-24), and electricity is bought from the main grid via the trading (Fig.8, intervals 1-10 and 22-24); On the contrary, at intervals 11-21, the power trading prices are high, PtH units are off with most of the power and heat energy generated by TG units. Further, in the electricity market, the MEMG will sell electricity at those intervals (Fig. 8).

ii) In the MEMG, the energy storage contributes to load leveling and shifting by the coordination with generators, market, and PtH units, in this way, the total multi-energy supply cost will be reduced: For EESs in Fig.8, they charge when power prices are low (i.e., intervals 4-6) and discharge when power prices are high (i.e., intervals 13-14, 20); Moreover, as there is degradation cost of the EES in (7), EESs would not charge or discharge too frequently. For the TES in Fig.9, all the heat energy stored will be released for the heat supply.

iii) The thermal inertia in the thermal network makes it a virtual energy storage. It can be seen from Fig.9 that the heat generation is not always equal to the demands, the difference means that the thermal network is absorbing or releasing heat. This storage will improve the operational flexibility of the MEMG and reduces holistic energy supply cost.

iv) Power trading is guided by the cost function of the MEMG operation in (2), after the trading, it can be seen in Fig.10 that the power prices are much smoother with fewer differences among all intervals. This is rational that the main grid and MEMG would negotiate with each other through the cooperative trading process on the prices to avoid too high or low prices.

The final MEMG multi-energy supply cost is 847.648 $ and the total solution time for the 24 rolling iterations is 4.087s with one horizon as only 0.170s. This computational performance shows the effectiveness of our MIQP problem.

5.3 Comparisons with Two Traditional Operation Benchmarks

In this section, to further show the effectiveness of our proposed method, comparison cases of our method with traditional MEMG operation benchmarks are conducted below:

Case 1: Non-cooperative operation: there is no market trading, that is, the MEMG is operated in the islanded mode, and the power and heat loads should be satisfied locally [4].

Case 2: Myopic operation [19]: the test MEMG operates with the instant updated information, i.e., the rolling horizon R^T is set as 1.

The final costs and computation time (for all 24 iterations) are given in Table. III. Note that for a clearer comparison, our test case is marked as **Case 3** in this table.

Table III: The MEMG configuration

Item	**Case 1**	**Case 2**	**Case 3**
Cost	1096.787$	877.976$	**847.648$**
Time	3.023s	3.353s	**4.087s**

From all the simulation results in Table. III, it can be inferred that:

i) *Power trading is essential for the MEMG to reduce its energy supply cost* as it could bring additional operation flexibility via the external energy resources from the main grid. Besides, the EES in the MEMG could make full use of the price differences to shift the loads and gain extra benefits. This verifies the significance of our cooperative trading model.

ii) *The dynamic rolling horizon strategy can be effective to reduce the cost under uncertainties from the renewable generation* compared with the myopic method. This is because it makes full use of all available information and will conduct more economic decisions. This piece of results validates the application of the dynamic rolling horizon method.

iii) Our proposed MIQP model is applicable for real-time MEMG operation. It can be seen that the computation time of all three cases is short and compatible with real-world applications.

All case studies in the Section.5 demonstrate the effectiveness of our method in this research in reducing MEMG multi-energy supply cost with a satisfactory solution performance.

6 Conclusion

In this paper, a cooperative MEMG operation method is proposed to reduce the energy supply cost. To tackle the stochasticity from renewable generation, the dynamic rolling horizon method is applied to fulfill the real-time multi-energy management with all the successively updated information. Through the effective coordination of all distributed units, a reliable and economic operation scheme is obtained with the below conclusions:

i) The cooperative MEMG operation model can be highly beneficial to reduce the overall energy supply cost as it brings extra electricity sources and operational flexibility.

ii) The dynamic rolling horizon strategy applied is effective in reducing the overall energy cost and immune against uncertainties as it can make the best of both the available short-lead-time and long-lead-time forecast information.

ii) Our problem modeling (MIQP) is practical for real-world applications since the finalized solution time is short.

For future work, firstly, to make full use of the historical data, data-driven-based methods such as the deep reinforcement learning method can be utilized [20]. Secondly, the gas network with hydrogen technology can be involved in this work for more comprehensive research [21]. At last, the electric vehicles which connect MEMG operations with the transportation network can also be included in future research [22].

References

[1]. C Klemm, P Vennemann.: Modeling and optimization of multi-energy systems in mixed-use districts: A review of existing methods and approaches. Renewable and Sustainable Energy Reviews, vol.135, pp. 110206, 2021.

[2]. T M Alabi, F D Agbajor, Z Yang, et al.: Strategic potential of multi-energy system towards carbon neutrality: A forward-looking overview. Energy and Built Environment, 2022.

[3]. C Lingmin, W Jiekang, W Fan, et al.: Energy flow optimization method for multi-energy system oriented to combined cooling, heating, and power. Energy, vol. 211, pp. 118536, 2020.

[4]. Z Li, Y Xu: Optimal coordinated energy dispatch of a multi-energy microgrid in grid-connected and islanded modes. Applied Energy, vol. 210, pp. 974-986, 2018.

[5]. S Mazzoni, et al.: Energy storage technologies as techno-economic parameters for master planning and optimal dispatch in smart multi-energy systems. Applied Energy, vol.254, pp. 113682, 2019.

[6]. H Qi, H Yue, J Zhang, et al: Optimisation of a smart energy hub with integration of combined heat and power, demand side response, and energy storage. Energy, vol. 234, pp. 121268, 2021.

[7]. M Mirzaei A, et al.: Evaluating the impact of multi-carrier energy storage systems in optimal operation of integrated electricity, gas, and district heating networks. Applied Thermal Engineering, vol.176, pp.115413, 2020.

[8]. Y Chen, et al.: Optimally coordinated dispatch of combined-heat-and-electrical network with demand response, IET Generation, Transmission & Distribution, vol.13, no.11, pp. 2216-2225, 2019.

[9]. Lu S, Gu W, Zhou J, et al.: Coordinated dispatch of multi-energy system with district heating network: Modeling and solution strategy. Energy, vol.152, pp. 358-370, 2018.

[10]. Z. Li, et al: Risk-Averse Coordinated Operation of a Multi-Energy Microgrid Considering Voltage/ Var Control and Thermal Flow: An Adaptive Stochastic Approach, IEEE Transactions on Smart Grid, vol. 12, no. 5, pp. 3914-3927, 2021

[11]. H Tan, W Yan, Z Ren, et al: A robust dispatch model for integrated electricity and heat networks considering price-based integrated demand response. Energy, vol. 239, pp. 121875, 2022.

[12]. J Zhong, et al: Distributed operation for integrated electricity and heat system with hybrid stochastic/robust optimization. International Journal of Electrical Power & Energy Systems, vol. 128, pp. 106680, 2021.

[13]. N Somu, G R MR, K Ramamritham, A hybrid model for building energy consumption forecasting using long short term memory networks. Applied Energy, vol. 261, pp. 114131, 2020.

[14]. T. Zhao, et al: Game theory based distributed energy trading for microgrid parks, 2017 Asian Conference on Energy, Power and Transportation Electrification (ACEPT), Singapore, pp. 1-7, 2017.

[15]. Z Wang, L Wang, Z Li, et al.: Optimal distributed transaction of multiple microgrids in grid-connected and islanded modes considering unit commitment scheme. International Journal of Electrical Power & Energy Systems, vol. 132, pp. 107146, 2021.

[16]. Y Chen, X Feng, Z Li, et al.: Multi-stage coordinated operation of a multi-energy

microgrid with residential demand response under diverse uncertainties. Energy Conversion and Economics, vol.1, no.1, pp. 20-33, 2020.
[17]. K V Konneh, et al.: Application Strategies of Model Predictive Control for the Design and Operations of Renewable EnergyBased Microgrid: A Survey. Electronics, vol. 11, no.4, pp.554, 2022.
[18]. D Das, H S Nagi, D P Kothari.: Novel method for solving radial distribution networks. IET Generation, Transmission & Distribution, vol.141, no.4, pp. 291-298, 1994. Proceedings, vol. 20, no..1, pp.39, 2022.
[19]. Z. Li, L. Wu, Y. Xu, S. Moazeni and Z. Tang: Multi-Stage Real-Time Operation of a Multi-Energy Microgrid With Electrical and Thermal Energy Storage Assets: A Data-Driven MPC-ADP Approach, IEEE Transactions on Smart Grid, vol. 13, no. 1, pp. 213-226, 2022.
[20]. Z. Yan and Y. Xu: Real-Time Optimal Power Flow: A Lagrangian Based Deep Reinforcement Learning Approach, IEEE Transactions on Power Systems, vol. 35, no. 4, pp. 3270-3273, 2020.
[21]. X Zheng, Y Xu, Z Li, et al: Co-optimisation and settlement of power-gas coupled system in day-ahead market under multiple uncertainties. IET Renewable Power Generation, vol.15, no.8, pp. 1632-1647, 2021.
[22]. N S Jayalakshmi, Jadoun V K, Gaonkar D N, etal.: Optimal operation of multi-source electric vehicle connected microgrid using metaheuristic algorithm. Journal of Energy Storage, vol.52, pp. 105067, 2022.